THE JOURNAL OF BIOLOGICAL CHEMISTRY VOL. 287, NO. 21, pp. 17198–17205, May 18, 2012

Conserved Asparagine Residue Located in Binding Pocket Controls Cation Selectivity and Substrate Interactions in Neuronal Glutamate Transporter*[S]

Received for publication, February 21, 2012, and in revised form, March 27, 2012 Published, JBC Papers in Press, April 4, 2012, DOI 10.1074/jbc.M112.355040

Shlomit Teichman, Shaogang Qu[1], and Baruch I. Kanner[2]

From the Department of Biochemistry and Molecular Biology, Institute for Medical Research Israel-Canada, Hebrew University Hadassah Medical School, Jerusalem 91120, Israel

Background: The cation binding sites of brain glutamate transporters are not yet identified.
Results: Mutation of a conserved asparagine residue changed cation selectivity and apparent substrate affinity.
Conclusion: This residue plays a crucial role in the ion-coupling mechanism of glutamate transporters.
Significance: The proposed direct coupling of the cation and solute fluxes may be relevant for other ion-coupled transporters.

Transporters of the major excitatory neurotransmitter glutamate play a crucial role in glutamatergic neurotransmission by removing their substrate from the synaptic cleft. The transport mechanism involves co-transport of glutamic acid with three Na^+ ions followed by countertransport of one K^+ ion. Structural work on the archeal homologue Glt_{Ph} indicates a role of a conserved asparagine in substrate binding. According to a recent proposal, this residue may also participate in a novel Na^+ binding site. In this study, we characterize mutants of this residue from the neuronal transporter EAAC1, Asn-451. None of the mutants, except for N451S, were able to exhibit transport. However, the K_m of this mutant for L-aspartate was increased ~30-fold. Remarkably, the increase for D-aspartate and L-glutamate was 250- and 400-fold, respectively. Moreover, the cation specificity of N451S was altered because sodium but not lithium could support transport. A similar change in cation specificity was observed with a mutant of a conserved threonine residue, T370S, also implicated to participate in the novel Na^+ site together with the bound substrate. In further contrast to the wild type transporter, only L-aspartate was able to activate the uncoupled anion conductance by N451S, but with an almost 1000-fold reduction in apparent affinity. Our results not only provide experimental support for the Na^+ site but also suggest a distinct orientation of the substrate in the binding pocket during the activation of the anion conductance.

Glutamate is the major excitatory neurotransmitter in the brain. Glutamate transporters move the transmitter from the synapse into the cells surrounding the synapse and thereby terminate the synaptic actions of this neurotransmitter. Glutamate transport is an electrogenic process (1–3), which consists of two half-cycles (4–6): (i) cotransport of the neurotransmitter with sodium and hydrogen ions (1, 7) and (ii) countertransport of potassium (1, 4). The stoichiometry is three sodium ions, one proton, and one potassium ion per transported glutamate molecule (8, 9). Glutamate transporters mediate two types of substrate-induced steady-state current: an inward-rectifying or "coupled" current, reflecting electrogenic ion-coupled glutamate translocation and an "uncoupled" sodium-dependent current, which is carried by chloride ions and further activated by the substrates of the transporter (10–12). Non-transportable substrate analogues, expected to "lock" the transporter in an outward-facing conformation when applied from the external side, are not only competitive inhibitors of the coupled current and of the substrate-induced uncoupled anion current but also inhibit the basal sodium-dependent anion conductance (13, 14).

The publication of the first high-resolution crystal structure of a glutamate transporter homologue, Glt_{Ph}, from the archeon *Pyrococcus horikoshii* represented a landmark for the field of glutamate transporters (15). The structure shows a trimer with a permeation pathway through each of the monomers, indicating that the monomer is the functional unit. This is also the case for the eukaryotic glutamate transporters (16–19). The membrane topology of the monomer (15) is quite unusual but is in excellent agreement with the topology inferred from biochemical studies (20–22). The monomer contains eight transmembrane domains (TMs)[3] and two oppositely oriented re-entrant loops, one between domains 6 and 7 (HP1) and the other between domains 7 and 8 (HP2). TMs 1–6 form the outer shell of the transporter monomer whereas TMs 7 and 8 and the two reentrant loops participate in the formation of the binding pocket of Glt_{Ph} (15, 23). Importantly, many of the amino acid residues of the transporter, inferred to be important in the interaction with sodium (24, 25), potassium (6, 26), and glutamate (27, 28) are facing toward the binding pocket. Recent studies indicate that glutamate translocation occurs by an "elevator-like" mechanism (29, 30) where the transport domain,

* This work was supported, in whole or in part, by the National Institutes of Neurological Disorders and Stroke through National Institutes of Health Grant NS 16708 and United States-Israel Binational Science Foundation Grant 2007051.
[S] This article contains supplemental Fig. 1.
[1] Present address: Dept. of Immunology, Southern Medical University, 1023 Shatai Rd. South, Guangzhou 510515, Guangdong, China.
[2] To whom correspondence should be addressed: Dept. of Biochemistry and Molecular Biology, Hebrew University Hadassah Medical School, P.O. Box 12272, Jerusalem 91120, Israel. Tel.: 972-2-6758506; Fax: 972-2-6757379; E-mail: kannerb@cc.huji.ac.il.

[3] The abbreviations used are TM, transmembrane domain; nA, nanoampere.

which includes HP1 and HP2 and TMs 3, 6, 7, and 8, moves relative to the fixed trimerization domain (31).

Because of the limited resolution of the Glt_{Ph} structure, Tl^+ ions, which exhibit a robust anomalous scattering signal, have been used in an attempt to visualize the sodium sites in this homologue (23), which also uses three Na^+ ions per transported substrate molecule (32). Two Tl^+ sites, proposed to represent Na^+ sites, were identified. However, in contrast to Na^+, Tl^+ could not support transport (23). Nevertheless, functional evidence supports the role of one of the Tl^+ sites (Na1) as a sodium binding site (33). In the absence of high-resolution structural data, suggestions for additional sodium binding sites have been searched by using a combination of computational and functional studies (34–36). Based on computational studies, the Na3 site was proposed to be formed by the side-chains of conserved threonine and asparagine residues, from TMs 7 and 8, respectively as well as by carboxyl oxygens of the acidic amino acid substrate (35). This proposal is attractive because it could explain the observation that the apparent affinity for different transported acidic amino acids depends on the nature of the cotransported cation (37).

However, although the analyzed mutants of the conserved asparagine (Asn-451 in the neuronal transporter EAAC1) could bind Na^+, they were transport-deficient (35). Thus, a possible role of the substrate in cation coordination at the Na3 site could not be probed. Here we report on an Asn-451 mutant, N451S, with significant transport activity. This transport has an altered selectivity not only for the cation but also for the substrate. Our data provide experimental support for the involvement of the substrate in the predicted Na3 site, providing an important clue for the coupling between cation and substrate fluxes. Moreover, the new data suggest a distinct orientation of the substrate in the binding pocket during the activation of the anion conductance.

EXPERIMENTAL PROCEDURES

Generation and Subcloning of Mutants—The C-terminal histidine-tagged versions of rabbit EAAC1 (EAAC1-WT) (38, 39) in the vector pBluescript SK^- (Stratagene) was used as a parent for site-directed mutagenesis (40, 41). This was followed by subcloning of the mutations into His-tagged EAAC1, residing in the oocyte expression vector pOG_2 (39), using the unique restriction enzymes NsiI and StuI. The subcloned DNA fragments were sequenced between these unique restriction sites.

cRNA Transcription, Injection, and Oocyte Preparation—For expression of wild type and mutant transporters, their cDNA constructs residing in the oocyte expression vector were linearized with SacI. Capped run-off cRNA transcripts were made from the transporter constructs using mMESSAGE-mMACHINE (Ambion). The transporter constructs were either EAAC1-WT (39) or the indicated mutants. The cRNAs were injected into *Xenopus laevis* oocytes, which were prepared as described (25), and transporter currents were measured 2–3 days post-injection, as described in the next paragraph.

Oocyte Electrophysiology—Oocytes were placed in the recording chamber, penetrated with two agarose-cushioned micropipettes (1%/2 M KCl, resistance varied between 1 and 3 megaohms), voltage clamped using GeneClamp 500 (Axon Instruments) and digitized using Digidata 1322 (Axon Instruments both controlled by the pClamp9.0 suite (Axon Instruments). Voltage jumping was performed using a conventional two-electrode voltage clamp as described previously (25). The standard buffer, termed ND96, was composed of 96 mM NaCl, 2 mM KCl, 1.8 mM $CaCl_2$, 1 mM $MgCl_2$, 5 mM Na-HEPES, pH 7.5. In sodium titration experiments, NaCl was replaced by equimolar concentrations of choline Cl. The composition of other perfusion solutions is indicated in the Fig. legends. Offset voltages in chloride substitution experiments were avoided by use of an agarose bridge (1%/2 M KCl) that connected the recording chamber to the Ag/AgCl ground electrode.

Data Analysis—All current-voltage relations represent steady-state substrate- elicited net currents ($(I_{buffer+substrate}) - (I_{buffer})$) and were analyzed by Clampfit (version 8.2 or 9.0, Axon instruments). Because of the variability in expression level within and between different oocyte batches, the data have been normalized as indicated in the figure legends. Kinetic parameters were determined by non-linear fitting to the generalized Hill equation using the built-in functions of Origin (version 6.1, Microcal). For determination of apparent affinity for substrate, the current observed at saturating substrate concentrations (I_{max}) and $K_{0.5}$ were allowed to vary and the value of n_H was fixed at 1. Because of the voltage dependence of I_{max}, we defined the kinetic parameters at −100 mV, except for Fig. 7, where the parameters were determined at +40 mV.

Cell Surface Biotinylation—To evaluate expression of the mutant transporters, biotinylation was done as described previously (36). Briefly, five oocytes expressing wild type or mutant EAAC1, were treated with 1.5 mg/ml of sulfosuccinimidyl-2-(biotinamide)ethyl-1,3-dithiopropionate (Pierce) dissolved in ND96. After solubilization of the membrane proteins with Triton X-100 and treatment with streptavidin beads, the biotinylated proteins were eluted with a final volume of 70 μl of SDS-PAGE sample buffer and analyzed by Western blotting. The blots were probed with an affinity purified antibody directed against rabbit EAAT3 (generously provided by N. C. Danbolt, University of Oslo; anti-C491 (Ab,371 (42)).

RESULTS

Transport and Surface Expression of Asn-451 Mutants—To test the role of the conserved asparagine residue, located at position 451 in EAAC1 in the transport mechanism, we measured the L-aspartate-induced transport currents in oocytes expressing the Asn-451 mutants in the presence of 96 mM Na^+. No measurable currents were seen with the alanine, cysteine, aspartate, and glutamine replacement mutants, even when L-aspartate was applied at 20 mM, a super-saturating concentration (Fig. 1*A*). However, at this concentration, the N451S mutant exhibited currents of a magnitude of ~60% of those by EAAC1-WT (Fig. 1*A*). These currents were not observed in the absence of sodium (replacement by choline; data not shown). The loss of activity of the N451A/N451C/N451D/N451Q mutants is not due to decreased steady-state levels of the mutant transporters on the plasma membrane because the intensity of the bands in the biotinylated fraction of these mutants is similar to that of EAAC1-WT or N451S, as shown by surface biotinylation (Fig. 1*B*).

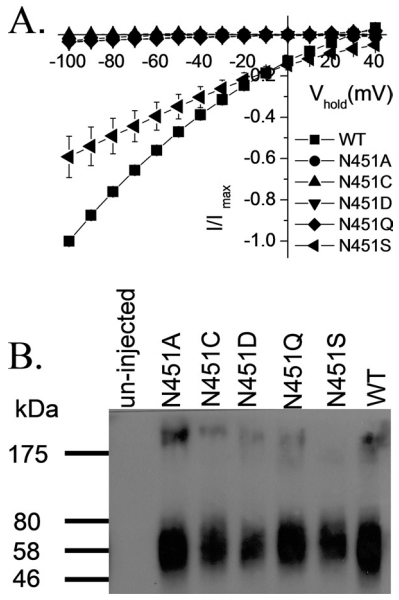

FIGURE 1. **Transport currents and surface expression of Asn-451 mutants.** *A*, oocytes expressing WT-EAAC1 or Asn-451 mutants were voltage clamped and gravity perfused with ND96 recording solution with and without 20 mM L-aspartate. The current in the absence of 20 mM L-aspartate was subtracted from that in its presence (*I*) and plotted against the holding potential (V_{hold}). The substrate-induced currents in oocytes expressing the mutants were normalized to currents at −100 mV measured in oocytes expressing EAAC1- WT from the same batch at the same day (I_{max}). The values shown are mean ± S.E. from three different batches. The currents at −100 mV induced by 20 mM L-aspartate ranged from −332 to −713 nA in the WT-EAAC1, from −1 to −34 nA in N451A, from 0 to −7 nA in N451C, from −5 to −40 nA in N451D, from −5 to −28 nA in N451Q and from −176 to −501 nA in N451S. *B*, *Xenopus* oocytes expressing EAAC1-WT and the indicated mutants were labeled and processed as described under "Experimental Procedures." The biotinylated samples are shown. The *left lane* shows a sample from non-injected oocytes. Marker proteins were run on the same gel, and their positions (in kDa) are indicated. The data are representative of three separate experiments.

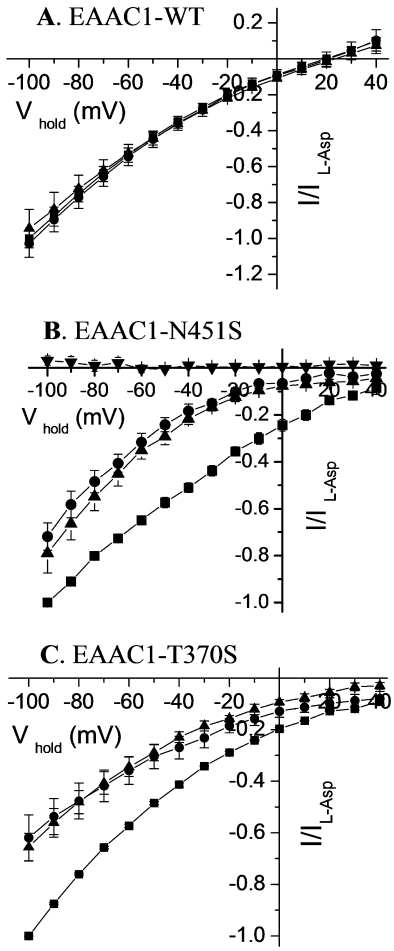

FIGURE 2. **Voltage dependence of the substrate-induced steady-state currents by EAAC1-WT, N451S, and T370S.** Steady-state currents induced by L-aspartate (*squares*), L-glutamate (*circles*), D-aspartate (*triangles*), or GABA (*inverted triangles*) are shown for EAAC1-WT (*A*), N451S (*B*), and T370S (*C*), using the substrates at 1, 20, and 5 mM, respectively were plotted against the holding potential (V_{hold}). The substrate-induced steady-state currents were obtained and analyzed as described in the legend to Fig. 1*A* and normalized to the current induced by L-aspartate at −100 mV ($I_{L\text{-}Asp}$). This voltage was used because the inward transport currents increase with the magnitude of the interior negative potential and voltages, which are more negative than −100 mV, were not always tolerated by the oocytes. Similar results were obtained at other membrane potentials more negative than −25 mV (the approximate reversal potential for chloride; not shown). The data are the means ± S.E. of at least four repeats. The magnitude of the currents induced by L-aspartate, L-glutamate, and D-aspartate at −100 mV ranged from −171 to −471 nA, −185 to −512 nA, and from −202 to −312 nA, respectively, for EAAC1-WT. For N451S, the corresponding values were from −85 to −223 nA, −58 to −172 nA, and from −52 to −169 nA, and for T370S from −224 to −410 nA, −142 to −195 nA, and −146 to −231 nA.

Substrate Specificity and Cation Selectivity of N451S—Because the Glt_{Ph} counterpart of Asn-451, Asn-401, directly coordinates the α-carboxylate group of L-aspartate (23), the voltage dependence of the currents induced by 20 mM of each of the substrates L-aspartate, D-aspartate, and L-glutamate was determined. In contrast to EAAC1-WT, where similar currents were elicited by each of these substrates (Fig. 2*A*), in the N451S mutant, larger currents were elicited by L-aspartate than by the two other substrates at all voltages (Fig. 2*B*). The substrate specificity of these measurements is illustrated by the fact that no currents were induced by GABA, which is not a substrate for the glutamate transporters (Fig. 2*B*).

The apparent substrate affinity of N451S for L-glutamate and D-aspartate was reduced much more dramatically than for L-aspartate (Fig. 3). The K_m values for the former two substrates were 3900 ± 424 and 2580 ± 82 μM, respectively, as compared with L-aspartate with a K_m of 308 ± 49 μM (n = 3) (Fig. 3). Nevertheless, also in the case of L-aspartate, there was a severe drop in apparent affinity because K_m values of ~10 μM for each of the three substrates were found for EAAC1-WT (37). Because of the high substrate concentration used in the experiments depicted in Fig. 2, each of the three substrates was saturating. The Glt_{Ph} counterpart of Thr-370, Thr-314, directly coordinates the β-carboxylate group of L-aspartate, rather than the α-carboxylate group coordinated by Glt_{Ph}-N401 (23). The only substitution mutant at position 370, which retains transport currents, is T370S (25). The currents induced by 5 mM of L-aspartate were also larger than those by L-glutamate or by D-aspartate (Fig. 2*C*).

In lithium-containing medium, significant L-aspartate-induced currents were observed by EAAC1-WT, albeit of smaller magnitude than in sodium (Fig. 4*A*). Also, L-glutamate and D-aspartate induced significant currents in oocytes expressing EAAC1-WT in lithium-containing media (Fig. 4*A*). We reported that the T370S mutant has an altered cation selectivity of radioactive transport and of the transport currents induced by L-aspartate (25). In contrast to EAAC1-WT, these activities were not seen with

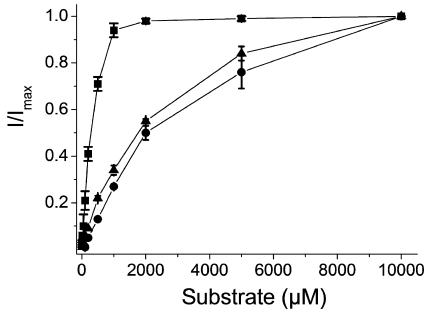

FIGURE 3. **Concentration dependence of substrate-induced currents mediated by N451S.** Steady-state currents induced by 10 mM of L-aspartate (*squares*), L-glutamate (*circles*), or D-aspartate (*triangles*) were obtained with oocytes expressing N451S. The currents were measured in ND96 at −100 mV. Substrate-induced currents were normalized separately for each substrate, and usually oocytes with higher expression levels were used for L-glutamate and D-aspartate than those used for L-aspartate. The data are the means ± S.E. of three repeats. The magnitude of the currents induced by L-aspartate, L-glutamate, and D-aspartate ranged from −132 to −460 nA, −108 to −366 nA, and −168 to −429 nA, respectively.

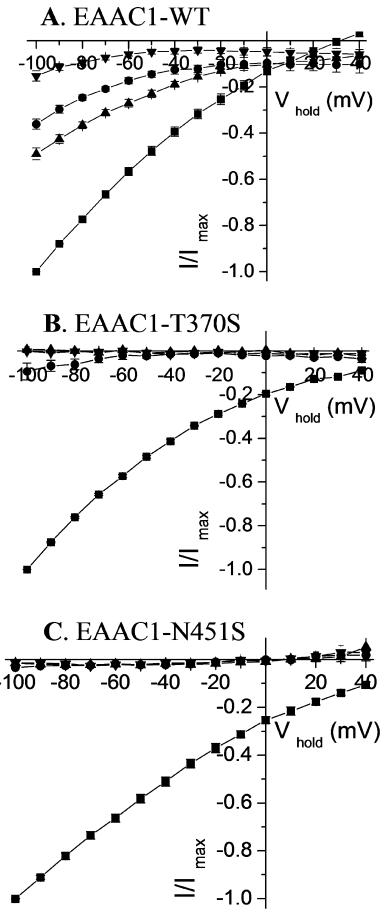

FIGURE 4. **Cation dependence of substrate-induced steady-state currents mediated by EAAC1-WT (*A*), T370S (*B*), and N451S (*C*) transporters.** The net currents in sodium induced by L-aspartate (*squares*) and in lithium (96 mM LiCl, 2 mM KCl, 1.8 mM $CaCl_2$, 1 mM $MgCl_2$, 5 mM Tris-HEPES, pH 7.5) by L-aspartate (*circles*), L-glutamate (*triangles*), and D-aspartate (*inverted triangles*) ranged between the following values, respectively: *A*, −251 to −580 nA, −79 to −224 nA, −115 to −273 nA, and −26 to −99 nA; *B*, −224 to −410 nA, −7 to −41 nA, 0 to −3 nA, and 0 to −2 nA; *C*, −194 to −407 nA, −3 to −14 nA, −1 to −7 nA, and 0 to −10 nA. All currents are normalized to those induced by L-aspartate in sodium at −100 mV. For WT-EAAC1 and N451S, the concentration of the substrates was 20 and 5 mM for T370S. Data are mean ± S.E. ($n = 3$).

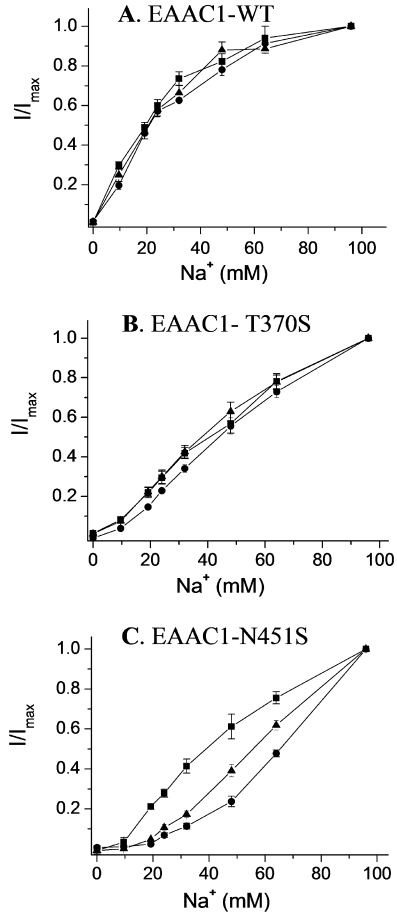

FIGURE 5. **Sodium concentration dependence of currents induced by substrates of EAAC1.** Steady-state currents induced by 20 mM of the substrates at −100 mV mediated by oocytes expressing EAAC1-WT (*A*), T370S (*B*), and N451S (*C*), were recorded at the indicated sodium concentrations (choline substitution). The currents are normalized separately for each substrate at 96 mM sodium (I/I_{max}). The currents induced by L-aspartate, L-glutamate, and D-aspartate, respectively ranged from: *A*, −45 to −297 nA, −58 to −357 nA, −33 to −305 nA; *B*, −134 to −380 nA, −80 to −541 nA, −88 to −640 nA; *C*, −92 to −581 nA, −111 to −344 nA, and −83 to −497 nA. The data are the means ± S.E. of at least three repeats.

the mutant in lithium (25). As can be seen in Fig. 4*B*, not only L-aspartate, but also D-aspartate and L-glutamate, were incapable of inducing any currents in the presence of lithium. Also in the case of the N451S mutant, none of the substrates induced any currents in the presence of this cation (Fig. 4*C*).

Sodium Concentration Dependence of Substrate-induced Currents—To examine whether the mutation has changed the affinity of the transporter for sodium in addition to the change in selectivity, we measured the sodium concentration dependence of currents induced by 20 mM of each of the substrates at −100 mV (Fig. 5). For EAAC1-WT, the concentration of sodium to obtain half-maximal activation of the currents was similar for all the substrates (22.8 ± 2.4, 26.8 ± 3.3, and 23.7 ± 2.6 mM for L-aspartate, L-glutamate, and D-aspartate, respectively (Fig. 5*A*)).

In the case of N451S, the apparent affinity for sodium was much lower than that of EAAC1-WT. In contrast to EAAC1-WT, no saturation was observed at 96 mM Na^+ (Fig. 5*C*). The sodium concentration dependence of the transport currents by N451S appeared dependent on the nature of the substrate and

half of the current measured at 96 mM was observed at ~40, 55, and 65 mM for L-aspartate, D-aspartate, and L-glutamate, respectively (Fig. 5*C*). However, even at 20 mM, D-aspartate and in particular L-glutamate are not saturating at 48 and 32 mM sodium any longer, in contrast to L-aspartate (data not shown). Thus, it is only possible to draw conclusions on the apparent sodium affinity in the case of L-aspartate. Clearly, the apparent affinity of N451S for sodium is reduced markedly in the presence of this substrate.

It has already been shown that T370S also has a decreased apparent affinity for sodium when the currents induced by L-aspartate are measured (25). Because of the differential effect of the substrates on the apparent affinity of sodium in N451S (Fig. 5*C*), it was important to determine whether this is also the case for T370S. The data shown in Fig. 5*B* demonstrate that the apparent sodium affinity of this mutant with the other two substrates was decreased as well, and no saturation by sodium was obtained for any of the three substrates.

Effects of N451S Mutation on Anion Conductance—Because the substrates not only induce the stoichiometric transport currents but also augment the "uncoupled" anion conductance (3, 10, 11), we investigated whether the decreased apparent substrate affinity of N451S is also seen when the anion conductance is monitored. To achieve this, 48 mM NaSCN was used to iso-osmotically replace half of the 96 mM NaCl. The conductance of thiocyanate is ~70-fold higher than that of chloride (43), and under these conditions, the substrate-induced currents are dominated by the anion conductance, especially at positive potentials. The outward currents at positive potentials reflect the entry of thiocyanate into the oocytes. In oocytes expressing EAAC1-WT, the three substrates induced similar currents in the presence of thiocyanate (Fig. 6*A*). In contrast, in the case of N451S, only L-aspartate induced robust currents at positive potentials (Fig. 6*B*). The corresponding currents induced by D-aspartate were diminished dramatically, and L-glutamate did not induce any currents in oocytes expressing N451S at positive potentials (Fig. 6*B*). The specificity of the substrate is illustrated by the fact that both with EAAC1-WT and N451S, GABA, also used at 20 mM, had only very small effects, if any (Fig. 6, *A* and *B*). The fact the blocker D,L-threo-β-benzyloxyaspartate, used at 600 μM, suppressed the anion conductance both in EAAC1-WT and in N451S (Fig. 6, *A* and *B*), indicates that the anion conductance *per se* is not altered in the mutant but merely its modulation by substrates.

Because of the results documented in Fig. 6*B*, the apparent substrate affinity of the induced anion conductance for N451S at +40 mV could only be determined for L-aspartate and the concentration giving a half-maximal effect was found to be 2.8 ± 0.4 mM (n = 3) (Fig. 7*A*), almost 10-fold higher than that of the coupled current (Fig. 3). However, with EAAC1-WT, the apparent affinity for the three substrates was similar to that of the coupled current, namely 3.2 ± 0.1, 4.3 ± 0.3 and 11.5 ± 1.2 μM (n = 3) for L-aspartate, D-aspartate, and L-glutamate, respectively (Fig. 7*C*). In the case of T370S, there was only a small differential effect on the voltage dependence of the currents induced by the substrates in the presence of thiocyanate (supplemental Fig. 1). Nevertheless, the apparent affinity for the substrates by T370S also was reduced markedly. The substrate concentrations giving a half maximal effect were 108 ± 17, 317 ± 14 and 1437 ± 135 μM for L-aspartate, D-aspartate, and L-glutamate, respectively (Fig. 7*B*).

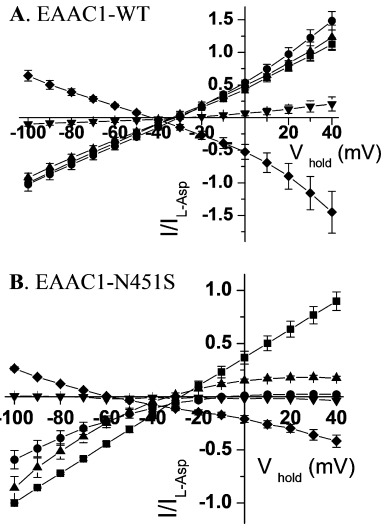

FIGURE 6. **Anion conductance by WT and N451S transporters.** Currents induced by 20 mm of L-aspartate (*squares*), L-glutamate (*circles*), D-aspartate (*triangles*), and GABA (*inverted triangles*) or suppressed by 600 μM D,L-threo-β-benzyloxyaspartate (*diamonds*), respectively, under conditions where half of the NaCl was replaced by an equimolar concentration of NaSCN are shown in oocytes expressing either WT-EAAC1 (*A*) or N451S (*B*). The currents in the absence of substrate/blocker were subtracted from those in its presence, normalized to the current induced by L-aspartate at −100 mV ($I_{L\text{-}Asp}$) and plotted against the holding potential (V_{hold}). The currents by L-aspartate, L-glutamate, D-aspartate, GABA, and D,L-threo-β-benzyloxyaspartate ranged from: *A*, −227 to −852 nA, −396 to −973 nA, −251 to −879 nA, −16 to −134 nA, and +151 to + 306 nA; and *B*, −86 to −512 nA, −120 to −328 nA, −126 to −559 nA, 0 to −5 nA, and +24 to +93 nA, respectively. Data shown are mean ± S.E. of four to five oocytes.

DISCUSSION

Except for substitution by serine, Asn-451 of the neuronal glutamate transporter EAAC1 is functionally irreplaceable (Fig. 1). Our finding that N451S exhibits transport activity enabled us to provide evidence that Asn-451 also controls substrate selectivity (Figs. 2, 3, 6, and 7), in addition to cation selectivity (Fig. 4). Such a change in cation selectivity, with L-aspartate as substrate, was shown originally for T370S (25). However, with N451Q, which was defective in transport, a decrease in the apparent affinity for both sodium and lithium was observed when the ability of these cations to induce conformational changes was monitored (35). In the case of EAAC1-WT, L-aspartate, L-glutamate, and D-aspartate exhibit similar K_m and I_{max} values (Fig. 2*A*) (37). The I_{max} of N451S for L-aspartate was somewhat higher than that of the other two substrates (Fig. 2*B*). However, the apparent affinity for the acidic amino acid substrates was decreased dramatically both in the absence or presence of thiocyanate (Figs. 3 and 7, respectively). This is in harmony with the observation that the α-carboxylate group of L-aspartate directly interacts with the corresponding asparagine residue (Asn-401) in Glt_{Ph} (23). Moreover, the apparent substrate affinity of N451S is not reduced to the same extent for each of the substrates: the interaction with D-aspartate and L-glutamate is more dramatically affected than with L-aspartate (Figs. 3 and 7). Apparently, the perturbation of the binding pocket differentially impairs the interactions of the three substrates.

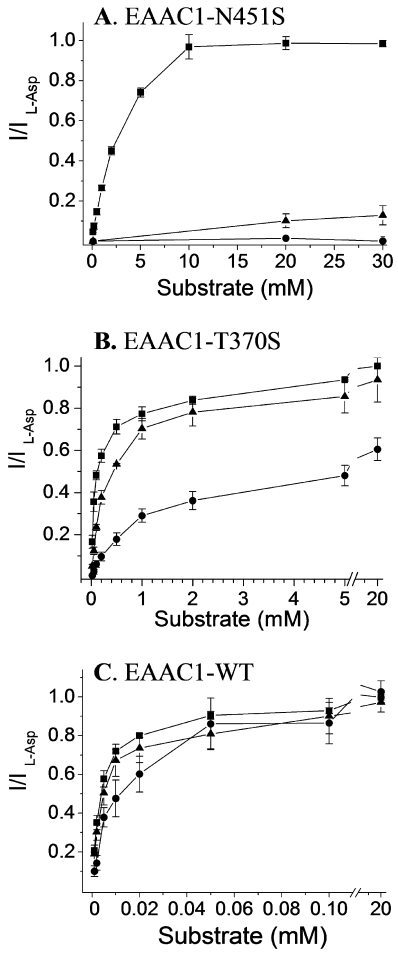

FIGURE 7. **Concentration dependence of substrate induced anion conductance of EAAC1-WT, T370S, and N451S.** Shown are steady-state currents by N451S (*A*), T370S (*B*), or EAAC1-WT (*C*) at +40 mV in a medium containing 48 mM SCN^- and 48 mM Cl^-, induced by either L-aspartate (*squares*), L-glutamate (*circles*), or D-aspartate (*triangles*), respectively, were measured. Substrate-induced currents were normalized to the L-aspartate currents at +40 mV. The currents (in nA) ranged from: *A*, +314 to +645, −17 to +29, and +10 to +105; *B*, +209 to +777, +104 to +522, and +239 to +627; *C*, +736 to 1719, +372 to +1036, and +301 to +952. The data are the means ± S.E. of three repeats. Note the different scales on the abscissa for the three panels.

We found that the most conservative substitutions of Asn-451, N451D, and N451Q, were deficient in transport (Fig. 1), and a similar observation for N451Q was made in another recent study (35). The lack of activity of the N451D mutant is probably due to the repulsion between the introduced negative charge and that of the α-carboxylate group of the substrate. Moreover, because the N451D mutation replaces the amide nitrogen by an oxygen atom, hydrogen bond formation is impaired. In the case of the N451Q mutation, the length of the side chain is increased, and this could be detrimental for the interaction of the amide group and the α-carboxylate group of the substrate. Because Asn-451, together with Thr-370, has been implicated in the interaction with the "third" Na^+, either directly and/or indirectly via the substrate (35), it is also possible that the lack of activity of N451Q may be due to an impaired Na^+ coordination. We reasoned that substitution of the asparagine by a shorter residue, which still has hydrogen bonding potential, may fulfill the requirements for transport. Indeed the N451S mutant exhibits significant transport (Fig. 1). In contrast to N451Q, which is only capable to perform sodium-induced conformational changes but cannot interact with the substrate (35), the N451S mutant represents a tool to probe the proposed role of the substrate at the Na3 site.

According to the current kinetic models of the glutamate transport cycle, two Na^+ bind before the acidic amino acid substrate followed by the binding of the third cation (44, 45). The finding that the apparent affinity for different transported amino acids depends on the nature of the co-transported cation (37), suggested the possibility that the substrate may participate directly in the coordination of the "third" Na^+ (or Li^+) in a similar way as has been shown for LeuT (46). The proposed Na3 site (35) is in perfect harmony with this idea. We found that in contrast to EAAC1-WT (Fig. 4*A*), Li^+ cannot support transport by N451S and only Na^+ can do so (Fig. 4*C*). This change in cation selectivity of substrate transport is consistent with the proposed Na3 site, although this does not rule out explanations involving long range effects of the mutation on a distant cation site. Nevertheless, it is striking that when Thr-370, which is also proposed to participate in the Na3 site, is mutated to serine a similar change in cation selectivity is observed ((25) and Fig. 4*B*)).

In addition to the changed cation selectivity of N451S, also the apparent Na^+ affinity of this mutant was decreased relative to EAAC1-WT (Fig. 5), at least when L-aspartate was the substrate. The apparent substrate affinity of T370S (25) is impacted less severely than that of N451S (Fig. 7), presumably because the T370S mutation is more conservative than the mutation of Asn-451 to serine. Therefore it is likely that the differential shift in the apparent affinity for Na^+ with the three substrates seen with N451S (Fig. 5*C*), is not observed with T370S (Fig. 5*B*). Despite this, the conservative T370S mutation nevertheless changes the cation selectivity of transport (Fig. 4*B*) (25).

All three substrates were able to activate the uncoupled anion conductance of EAAC1-WT (Fig. 6*A*), but in the case of N451S, only L-aspartate could do so at the testable concentrations (Fig. 6*B*). In contrast to the 30-fold reduction in apparent affinity for L-aspartate by N451S in the presence of chloride (Fig. 3), an almost 1000-fold reduction in apparent affinity was seen monitoring the activation of the anion conductance (Fig. 7, *A* and *C*). It is possible that L-glutamate and D-aspartate are capable of stimulating the anion conductance. However, their apparent affinity is so low that it is not possible to detect it at usable concentrations. In the case of the more conservative T370S mutation, the apparent substrate affinities were also reduced, but to a lesser extent than with N451S (Fig. 7*B*). The results suggest that the interaction of the substrate with the binding pocket during the activation of the uncoupled anion conductance, is different from that required during coupled transport. The distinct cation specificity of the anion conductance in EAAC1-WT (25) and the properties of mutants, where transportable substrates become inhibitors of the anion conductance (28, 47), are consistent with the idea of such a differential interaction.

Acknowledgment—We thank Niels C. Danbolt for the affinity purified antibody against EAAC1.

REFERENCES

1. Kanner, B. I., and Sharon, I. (1978) Active transport of L-glutamate by membrane vesicles isolated from rat brain. *Biochemistry* **17,** 3949–3953
2. Brew, H., and Attwell, D. (1987) Electrogenic glutamate uptake is a major current carrier in the membrane of axolotl retinal glial cells. *Nature* **327,** 707–709
3. Wadiche, J. I., Arriza, J. L., Amara, S. G., and Kavanaugh, M. P. (1995) Kinetics of a human glutamate transporter. *Neuron* **14,** 1019–1027
4. Kanner, B. I., and Bendahan, A. (1982) Binding order of substrates to the sodium and potassium ion coupled L-glutamic acid transporter from rat brain. *Biochemistry* **21,** 6327–6330
5. Pines, G., and Kanner, B. I. (1990) Counterflow of L-glutamate in plasma membrane vesicles and reconstituted preparations from rat brain. *Biochemistry* **29,** 11209–11214
6. Kavanaugh, M. P., Bendahan, A., Zerangue, N., Zhang, Y., and Kanner, B. I. (1997) Mutation of an amino acid residue influencing potassium coupling in the glutamate transporter GLT-1 induces obligate exchange. *J. Biol. Chem.* **272,** 1703–1708
7. Nelson, P. J., Dean, G. E., Aronson, P. S., and Rudnick, G. (1983) Hydrogen ion cotransport by the renal brush border glutamate transporter. *Biochemistry* **22,** 5459–5463
8. Zerangue, N., and Kavanaugh, M. P. (1996) Flux coupling in a neuronal glutamate transporter. *Nature* **383,** 634–637
9. Levy, L. M., Warr, O., and Attwell, D. (1998) Stoichiometry of the glial glutamate transporter GLT-1 expressed inducibly in a Chinese hamster ovary cell line selected for low endogenous Na^+-dependent glutamate uptake. *J. Neurosci.* **18,** 9620–9628
10. Wadiche, J. I., Amara, S. G., and Kavanaugh, M. P. (1995) Ion fluxes associated with excitatory amino acid transport. *Neuron* **15,** 721–728
11. Fairman, W. A., Vandenberg, R. J., Arriza, J. L., Kavanaugh, M. P., and Amara, S. G. (1995) An excitatory amino-acid transporter with properties of a ligand-gated chloride channel. *Nature* **375,** 599–603
12. Arriza, J. L., Eliasof, S., Kavanaugh, M. P., and Amara, S. G. (1997) Excitatory amino acid transporter 5, a retinal glutamate transporter coupled to a chloride conductance. *Proc. Natl. Acad. Sci. U.S.A.* **94,** 4155–4160
13. Otis, T. S., and Kavanaugh, M. P. (2000) Isolation of current components and partial reaction cycles in the glial glutamate transporter EAAT2. *J. Neurosci.* **20,** 2749–2757
14. Grewer, C., Watzke, N., Wiessner, M., and Rauen, T. (2000) Glutamate translocation of the neuronal glutamate transporter EAAC1 occurs within milliseconds. *Proc. Natl. Acad. Sci. U.S.A.* **97,** 9706–9711
15. Yernool, D., Boudker, O., Jin, Y., and Gouaux, E. (2004) Structure of a glutamate transporter homologue from *Pyrococcus horikoshii*. *Nature* **431,** 811–818
16. Koch, H. P., and Larsson, H. P. (2005) Small-scale molecular motions accomplish glutamate uptake in human glutamate transporters. *J. Neurosci.* **25,** 1730–1736
17. Grewer, C., Balani, P., Weidenfeller, C., Bartusel, T., Tao, Z., and Rauen, T. (2005) Individual subunits of the glutamate transporter EAAC1 homotrimer function independently of each other. *Biochemistry* **44,** 11913–11923
18. Leary, G. P., Stone, E. F., Holley, D. C., and Kavanaugh, M. P. (2007) The glutamate and chloride permeation pathways are colocalized in individual neuronal glutamate transporter subunits. *J. Neurosci.* **27,** 2938–2942
19. Koch, H. P., Brown, R. L., and Larsson, H. P. (2007) The glutamate-activated anion conductance in excitatory amino acid transporters is gated independently by the individual subunits. *J. Neurosci.* **27,** 2943–2947
20. Grunewald, M., Bendahan, A., and Kanner, B. I. (1998) Biotinylation of single cysteine mutants of the glutamate transporter GLT-1 from rat brain reveals its unusual topology. *Neuron* **21,** 623–632
21. Grunewald, M., and Kanner, B. I. (2000) The accessibility of a novel reentrant loop of the glutamate transporter GLT-1 is restricted by its substrate. *J. Biol. Chem.* **275,** 9684–9689
22. Slotboom, D. J., Sobczak, I., Konings, W. N., and Lolkema, J. S. (1999) A conserved serine-rich stretch in the glutamate transporter family forms a substrate-sensitive reentrant loop. *Proc. Natl. Acad. Sci. U.S.A.* **96,** 14282–14287
23. Boudker, O., Ryan, R. M., Yernool, D., Shimamoto, K., and Gouaux, E. (2007) Coupling substrate and ion binding to extracellular gate of a sodium-dependent aspartate transporter. *Nature* **445,** 387–393
24. Zhang, Y., and Kanner, B. I. (1999) Two serine residues of the glutamate transporter GLT-1 are crucial for coupling the fluxes of sodium and the neurotransmitter. *Proc. Natl. Acad. Sci. U.S.A.* **96,** 1710–1715
25. Borre, L., and Kanner, B. I. (2001) Coupled, but not uncoupled, fluxes in a neuronal glutamate transporter can be activated by lithium ions. *J. Biol. Chem.* **276,** 40396–40401
26. Zhang, Y., Bendahan, A., Zarbiv, R., Kavanaugh, M. P., and Kanner, B. I. (1998) Molecular determinant of ion selectivity of a (Na^+ + K^+)-coupled rat brain glutamate transporter. *Proc. Natl. Acad. Sci. U.S.A.* **95,** 751–755
27. Bendahan, A., Armon, A., Madani, N., Kavanaugh, M. P., and Kanner, B. I. (2000) Arginine 447 plays a pivotal role in substrate interactions in a neuronal glutamate transporter. *J. Biol. Chem.* **275,** 37436–37442
28. Teichman, S., and Kanner, B. I. (2007) Aspartate 444 is essential for productive substrate interactions in a neuronal glutamate transporter. *J. Gen. Physiol.* **129,** 527–539
29. Reyes, N., Ginter, C., and Boudker, O. (2009) Transport mechanism of a bacterial homologue of glutamate transporters. *Nature* **462,** 880–885
30. Crisman, T. J., Qu, S., Kanner, B. I., and Forrest, L. R. (2009) Inward-facing conformation of glutamate transporters as revealed by their inverted topology structural repeats. *Proc. Natl. Acad. Sci. U.S.A.* **106,** 20752–20757
31. Groeneveld, M., and Slotboom, D. J. (2007) Rigidity of the subunit interfaces of the trimeric glutamate transporter GltT during translocation. *J. Mol. Biol.* **372,** 565–570
32. Groeneveld, M., and Slotboom, D. J. (2010) Na^+:Aspartate coupling stoichiometry in the glutamate transporter homologue Glt_{Ph}. *Biochemistry* **49,** 3511–3513
33. Teichman, S., Qu, S., and Kanner, B. I. (2009) The equivalent of a thallium binding residue from an archeal homologue controls cation interactions in brain glutamate transporters. *Proc. Natl. Acad. Sci. U.S.A.* **106,** 14297–14302
34. Tao, Z., Rosental, N., Kanner, B. I., Gameiro, A., Mwaura, J., and Grewer, C. (2010) Mechanism of cation binding to the glutamate transporter EAAC1 probed with mutation of the conserved amino acid residue Thr-101. *J. Biol. Chem.* **285,** 17725–17733
35. Larsson, H. P., Wang, X., Lev, B., Baconguis, I., Caplan, D. A., Vyleta, N. P., Koch, H. P., Diez-Sampedro, A., and Noskov, S. Y. (2010) Evidence for a third sodium-binding site in glutamate transporters suggests an ion/substrate coupling model. *Proc. Natl. Acad. Sci. U.S.A.* **107,** 13912–13917
36. Rosental, N., Bendahan, A., and Kanner, B. I. (2006) Multiple consequences of mutating two conserved β-bridge forming residues in the translocation cycle of a neuronal glutamate transporter. *J. Biol. Chem.* **281,** 27905–27915
37. Menaker, D., Bendahan, A., and Kanner, B. I. (2006) The substrate specificity of a neuronal glutamate transporter is determined by the nature of the coupling ion. *J. Neurochem.* **99,** 20–28
38. Kanai, Y., and Hediger, M. A. (1992) Primary structure and functional characterization of a high-affinity glutamate transporter. *Nature* **360,** 467–471
39. Borre, L., and Kanner, B. I. (2004) Arginine 445 controls the coupling between glutamate and cations in the neuronal transporter EAAC-1. *J. Biol. Chem.* **279,** 2513–2519
40. Pines, G., Zhang, Y., and Kanner, B. I. (1995) Glutamate 404 is involved in the substrate discrimination of GLT-1, a (Na^+ + K^+)-coupled glutamate transporter from rat brain. *J. Biol. Chem.* **270,** 17093–17097
41. Kunkel, T. A., Roberts, J. D., and Zakour, R. A. (1987) Rapid and efficient site-specific mutagenesis without phenotypic selection. *Methods Enzymol.* **154,** 367–382
42. Holmseth, S., Dehnes, Y., Bjørnsen, L. P., Boulland, J. L., Furness, D. N., Bergles, D., and Danbolt, N. C. (2005) Specificity of antibodies: Unexpected cross-reactivity of antibodies directed against the excitatory amino acid transporter 3 (EAAT3). *Neuroscience* **136,** 649–660
43. Wadiche, J. I., and Kavanaugh, M. P. (1998) Macroscopic and microscopic properties of a cloned glutamate transporter/chloride channel. *J. Neurosci.* **18,** 7650–7661

44. Watzke, N., Bamberg, E., and Grewer, C. (2001) Early intermediates in the transport cycle of the neuronal excitatory amino acid carrier EAAC1. *J. Gen. Physiol.* **117,** 547–562
45. Bergles, D. E., Tzingounis, A. V., and Jahr, C. E. (2002) Comparison of coupled and uncoupled currents during glutamate uptake by GLT-1 transporters. *J. Neurosci.* **22,** 10153–10162
46. Yamashita, A., Singh, S. K., Kawate, T., Jin, Y., and Gouaux, E. (2005) Crystal structure of a bacterial homologue of Na^+/Cl-dependent neurotransmitter transporters. *Nature* **437,** 215–223
47. Rosental, N., and Kanner, B. I. (2010) A conserved methionine residue controls the substrate selectivity of a neuronal glutamate transporter. *J. Biol. Chem.* **285,** 21241–21248